J Therm Anal Calorim (2009) 97:775–780
DOI 10.1007/s10973-009-0330-y

Sintering studies on Ni–Cu–YSZ SOFC anode cermet processed by mechanical alloying

Thomaz Augusto Guisard Restivo · Sonia Regina Homem Mello-Castanho

ICTAC2008 Conference

Abstract New 40 vol%[(Cu)–Ni]–YSZ cermet materials processed by mechanical alloying (MA) of the row powders are prepared. The powder compacts are sintered in air, hydrogen and inert (argon) atmospheres at a dilatometer and tubular furnace up to 1,350 °C. Sintering by activated surface concept (SAS) can anticipate and enhance the densification in such powders. Stepwise isothermal dilatometry (SID) sintering kinetics study is performed allowing determining kinetic parameters for Ni–YSZ and Ni–Cu–YSZ pellets. Two-steps sintering processes is indicated while Cu-bearing material features the smallest activation energy for sintering. The allied MA–SAS method is a promising route to prepare SOFC fuel cell anode materials.

Keywords Fuel cell · Sintering kinetics · SOFC anode

Introduction

Solid oxide fuel cells (SOFC) is one of the most promised technologies to take part at electrical energy generation systems world wide due to its high conversion efficiency, energy output and low pollutant release. Among SOFC components, the anode has outstanding functions including fuel oxidation, electronic conductivity, O^{2-} ion transport and great flexibility regarding the direct use of bio and fossil fuels. SOFC technology is especially attractive for Brazilian energetic matrix due to the actual structure for ethanol production and distribution. However, technical problems related to poisoning by carbon deposition at the anode still remain, avoiding broad alcohol fuels utilization. If low steam content is present at the anode, the reforming product CO can be reversed to carbon which may block active sites and pores, degrading anode performance [1]. The mechanisms of carbon deposition, which arises from fuel reforming and Boudouard reaction, involve C solving in Ni lattice and further precipitation as filaments that cover the metal surface and pores [2, 3], reducing drastically the cell power output.

The conventional preparation route for Ni–YSZ anodes consists on mixing YSZ and NiO powders followed by sintering in an oxidant atmosphere and reduction at 900–1,000 °C in a further process step or in situ by the fuel in the SOFC [1, 4, 5]. The shrinkage produced by the reduction of NiO to Ni is rather small. A common practice is to include pore-forming additives, like graphite, in order to reach a suitable porosity range for gas flow (nearly 40%) [4].

The mechanical alloying (MA) process is investigated in the present work as a means to obtain directly the SOFC anode material from YSZ and metallic Ni powders, avoiding pore-forming aids and subsequent reduction operations. The method is also envisioned as a way to add metallic additives efficiently, like Cu, to increase the anode tolerance to C-bearing fuels [5, 6]. Implementing in parallel, the MA high energy milling can give rise to the sintering by activated surface method (SAS), where fresh surfaces are created during milling operation and further during heating cycle. The SAS concept foresees the increasing of the sinterability of the powders leading to anticipated retraction onset temperature [7].

The main tool employed for evaluation of the powders sinterability is the stepwise isothermal dilatometry (SID) approach. The SID method is a quasi-isothermal analysis

T. A. G. Restivo (✉) · S. R. H. Mello-Castanho
Centro de Ciências e Tecnologia de Materiais – CCTM – IPEN,
Cidade Universitária, Av. Lineu Prestes 2242,
05508000 São Paulo, SP, Brazil
e-mail: guisard@dglnet.com.br

S. R. H. Mello-Castanho
e-mail: srmello@ipen.br

where the kinetic parameters can be determined in one sole experiment as a function of the temperature [8–12]. Several isotherms distributed along the heating cycle within the relevant temperature range are generally imposed to accomplish the SID analysis.

Sintering kinetics theory

Some equations were attempted in order to fit the shrinkage data registered during sintering, leading to calculate the activation energy. The first one was derived from the basic equation for the shrinkage related to time [13–15]:

$$\Delta L/L_o = y = [K(T) \cdot t]^n \quad (1)$$

were K(T) is analogous to reaction rate constant and n is a parameter related to the mechanism, equivalent to reaction order. To apply for the dilatometric data Eq. 1 should be used into the differential form:

$$\ln(dy/dt) = \ln[n \cdot K(T)] - (1/n - 1) \ln y \quad (2)$$

Assuming the sintering process as isotropic, the normalized volumetric shrinkage can be expressed as $Y = (V_o - V_t)/(V_o - V_f) = (L_o^3 - L_t^3)/(L_o^3 - L_f^3)$, where the subscriptions o, t and f mean the dimension values at the beginning, at a time t and at the end of the sintering. Replacing the relative linear shrinkage $\Delta L/L_o$ in the Eq. 1 by the relative volumetric shrinkage $Y/(1 - Y) = (V_o - V_t)/(V_t - V_f)$, followed by differentiation on time, a normalized shrinkage equation can be developed [16, 17]:

$$dY/dt = nK(T)Y(1 - Y)[(1 - Y)/Y]^{1/n} \quad (3)$$

At any isotherm, the Plot $\ln\{(dY/dt)[1/Y(1 - Y)]\}$ versus $\ln[(1 - Y)/Y]$ yields a straight line from what n and K(T) are calculated. The rate constant parameter obeys the Arrhenius Equation:

$$K(T) = A \cdot \exp(-Q/RT) \Rightarrow \ln[K(T)] = \ln A - Q/RT \quad (4)$$

Therefore, the apparent activation energy Q can be determined from the plot $\ln[K(T)] \times 1/T$.

Experimental

Starting powders were YSZ (cubic zirconia, 8 mol%Y_2O_3, Tosoh Corp.), metallic Ni with 28 μm average particle size (CIRQ Cromato, 400 mesh, 99,6 mass% purity) and a 3 μm-Cu powder exceeding 99.9 mass% purity. The 40 vol%metal-YSZ samples were prepared by high energy milling in a shaker mill (SPEX 8000) at a rotation speed of 19 Hz for 1 to 8-h periods. Ultra-high molecular mass (UHMW) polyethylene and PTFE vials were used in a milling medium of 5 mm diameter tetragonal zirconia YTZ spheres. Another experimental set was performed employing vanadium hard steel (VC131) vial and 5 mm diameter 52100 grade steel spheres. The balls-to-powder mass ratio was 10:1 for a total powder mass of 10 g. For purposes of comparison, two samples—40 vol%Ni–YSZ and 55 vol%NiO–YSZ—were prepared by mixing and homogenizing the raw powders in alcohol slurries, and the former is referred to as homogenized cermet. MA was performed under air once a previous study [7] has demonstrated the milling atmosphere inside the vials has little influence since the powder oxidation level was negligible. The powder samples were subjected to uniaxial pressing at 150 MPa to conform 7 mm diameter pellets. The pellets were sintered in air and argon flowing gases both in a muffle furnace and in a vertical dilatometer/TMA (Setaram Labsys TMA 1,400 °C). The heating rate was 10 °C/min up to 1,300 and 1,350 °C and dwelling time of 0.5 and 1 h. SID heating cycles used the same heating rate while several isotherms were programmed at each 50 °C, from 200 °C up to 1,200 °C. The TMA load for all experiments was set at 2 g in order to cause no influence on sintering profiles. Also the required isotropic assumption for SID kinetic evaluation is especially valid at low load level attained in a vertical dilatometer like the one presently used. One sample was analyzed by simultaneous TG/DTA up to 1,200 °C (Setaram Labsys TG/DTA 1,600 °C) to give more assertions regarding the phenomena talking place during sintering.

Results and discussion

Mechanical alloying yields fine Ni–YSZ powders with mean particle size approaching 5 μm after 2-h processing time [7]. The primary crystallite sizes are in the nanometric range, as seen by SEM and TEM images in Fig. 1. The aggregates are composed by YSZ particles embedded on deformed Ni into a layered morphology. Previous works has demonstrated the constituents are intimate mixed in a very refined lamellar morphology possessing a highly defective structure [17].

Conventional sintering study in air is shown in Fig. 2 for 40 vol% Ni–YSZ and 40 vol%(Cu–Ni)–YSZ samples subjected to MA during 2 h. In the last sample, Cu was added to replace 50 vol% of Ni. Homogenized Ni–YSZ and oxide based NiO–YSZ samples are also included for comparison. It can be seen the sample pellets containing metals undergo first an expansion due to oxidation, followed by the sintering retraction. Retraction onset temperature of 950 °C is similar for YSZ, NiO–YSZ and for the homogenized cermet samples. By examining the point where the expansion is cancelled by the shrinkage, one can verify the materials subjected to MA have lower onset temperatures, specially the Cu-bearing Ni–YSZ sample.

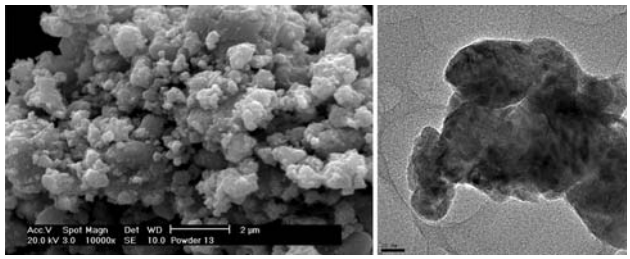

Fig. 1 MA processed Ni–YSZ powder images: SEM SE (*left*), TEM (*right*)

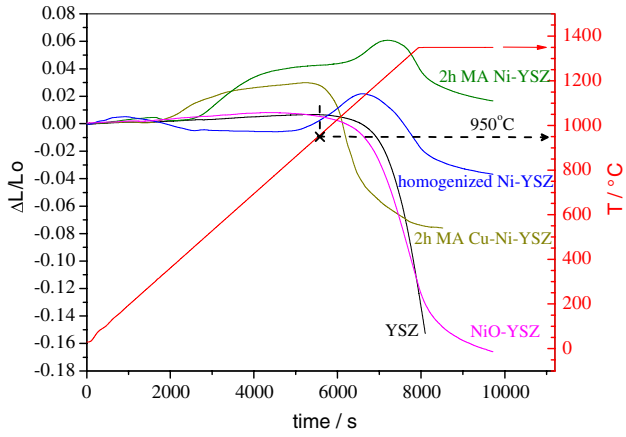

Fig. 2 Dilatometric sintering profiles under air atmosphere

The sintering behavior of Ni–YSZ MA samples under inert atmosphere (argon) up to 1,300 °C (Fig. 3) is similar, except for the expansion due to the oxidation. The higher the MA processing time and hence the energy delivered, the lower the initial sintering temperature. In the present case, a start sintering temperature as low as 195 °C was registered for 8 h MA Ni–YSZ powder compact. However, the total shrinkage is smaller for MA processed powder pellets compared to the homogenized Ni–YSZ one. In both sintering conditions, total densification was inhibited compared to the YSZ and NiO–YSZ samples. In [18] the sintering of Ni metal is inhibited in the presence of thin ceramic particles, as in the case of reinforced cermets. In contrast, very thin and highly deformed Ni particles are reported to bring on sintering at temperatures below 200 °C [19, 20]. The balance between these effects may explain the actual behavior during the sintering process. Actually, the lower densification is beneficial to anode material preparation process, once pore-forming additives are dispensed and the cermet can be obtained directly with Ni in the metallic form and proper porosity. Final density compilation for sintered pellets resulted in the 60–70%TD range.

The behavior of 8 h MA Ni–YSZ powder compact was further investigated by TG/DTA in the same conditions as the dilatometric analysis, allowing coupling all the signals in Fig. 4. It can be noted by the shrinkage rate curve that the

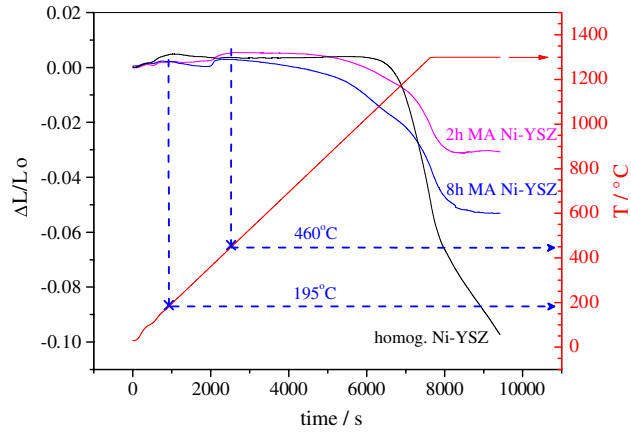

Fig. 3 Sintering profiles under argon; the onset temperatures are highlighted

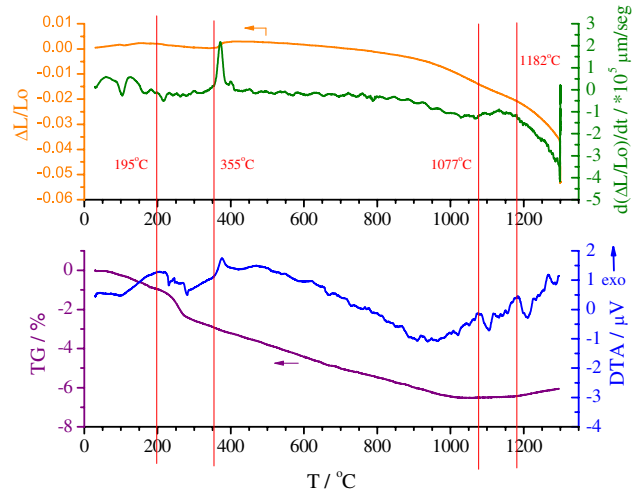

Fig. 4 TG/DTA and dilatometric curve coupled for Ni–YSZ powder pellet processed by MA during 8 h

sintering onset takes place at low temperature, immediately followed by a mass loss indicating the decomposition of polymer contamination from the UHMW milling container. An exothermic peak is assigned at 355 °C with a corresponding local expansion, which can be interpreted as the recrystallization of Ni. Afterwards the solid state sintering is resumed. The presence of two endothermic peaks of melting at 1,077 and 1,182 °C suggests the liquid phase sintering process can occur to accelerate the retraction. The carbon pickup of this powder was measured as 2.5% by LECO analyzer, which means the Ni–C eutectic alloy can be formed, leading to some liquid phase, even in small amounts. The X-ray diffraction patterns shown in Fig. 5 support these findings, once the Ni reflections were strongly shifted and traces of Ni_3C are identified in the powder after 8 h MA into an UHMW vial. The Ni_3C compound is normally formed from the C supersaturated Ni solution at 318 °C on heating, undergoing decomposition at 460 °C, as

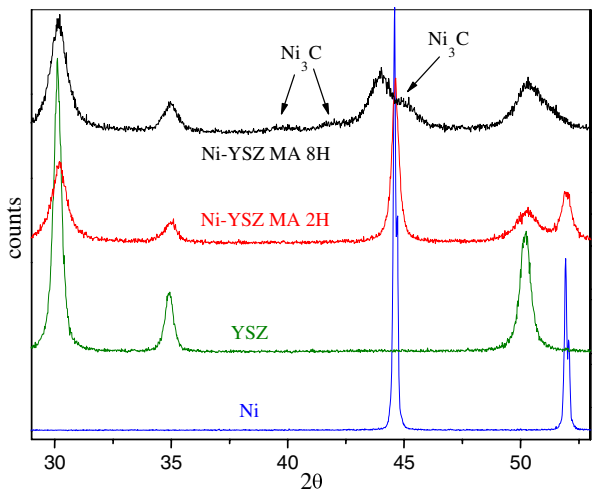

Fig. 5 X-ray diffraction profiles of the row powders and MA processed for 2 and 8 h

stated in [21], with good agreement with the present sintering curves. It appears the MA process is enough energetic to cause Ni_3C to form earlier in the powder. The MA performed into PTFE vials was successful to reduce the C pickup at about 50%, especially at 2 h MA processed powders, while the decreasing for 8 h duration is marginal. The reduction of the initial sintering temperature of the MA samples indicates the process is enhanced by active surface, which may be formed during the milling process, but also during sintering heating cycle. The MA process produces a slight oxidation on metallic surfaces, among them thin NiO layers can be removed during heating releasing the active surfaces to sinter, according to the SAS concept. The considered mechanisms of SAS include evaporation, solving in the matrix and reactive sintering, presently under study.

SID kinetic analysis

A typical SID kinetic analysis curve up to 1,200 °C for this study is shown in Fig. 6, which has been also processed according to Eq. 3, yielding some linear plots with 1/n slopes. The rate constants K(T) calculated at each established isotherm allow to build the Arrhenius plot ln(K(T)) × 1/T for the materials from where the activation energies are derived. It should be noted that each K(T) value results from the computation of about 200 aligned data points recorded at the dilatometer. The three plots at Fig. 7 are scaled equally in order to demonstrate the different slopes related to activation energies together with the respective fitting uncertainties. The straight plots obtained with only two points are merely indicative of a tendency for activation energy values and then dashed lines are drawn. The determined activation energy is clearly smaller for the Cu doped Ni–YSZ material and also rather inferior

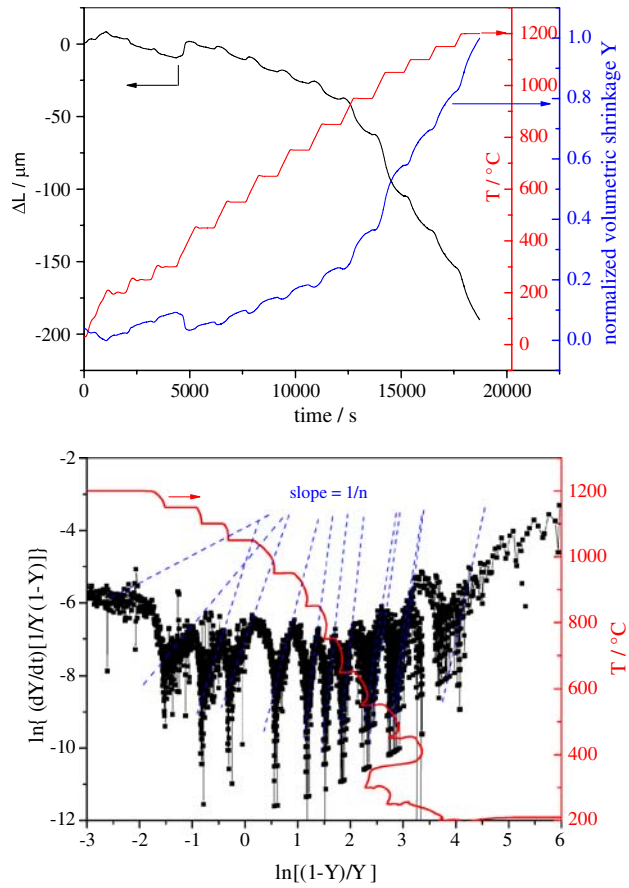

Fig. 6 SID kinetic cycle for Ni–YSZ MA sample (*left*); data treatment according Eq. 3 (*right*)

for MA Ni–YSZ, compared to the homogenized sample, suggesting the sintering process is favored.

It appears the sintering process mechanisms change two times, from small activation energies to higher ones, implying it happens through a 2-step process. It has been suggested the process is initially controlled by Ni (Cu) sintering, which explains the smaller values at low temperature. Afterwards, the process control is assumed by YSZ particles sintering at increased activation energies. It should be noted the MA processed powders have sintered at lower temperatures, specially for 8 h MA powder, where the second step related to YSZ sintering is anticipated to 750 °C. Comparing to conventional YSZ sintering onset (950 °C, Fig. 2), there is an important gain regarding the reduction of sintering temperature. The SID analysis of the as received pure YSZ powder compacts and milled for 2 h can give more assertions on the sintering process control, as shown in Fig. 8. The activation energy for the MA 2 h processed YSZ green pellet is smaller compared to the not-milled one, suggesting the high energy milling process may increase the sinterability of such powders. Moreover, the initial temperature of sintering is lowered from 950 °C down to 450 °C, where the milled powder starts to sinter slowly.

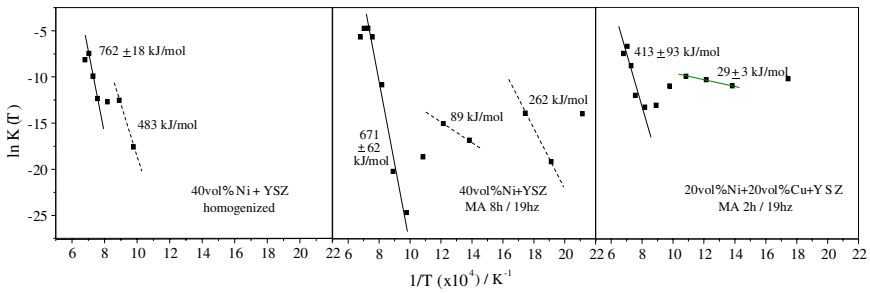

Fig. 7 Apparent activation energies for sintering determined by SID method for MA 40 vol%metal-YSZ cermets: homogenized, Ni–YSZ and Cu doped Ni–YSZ (from *left* to the *right*); polymer vials

The sintering activation energy evaluation for sample milled in steel vials is shown in Fig. 9. In these cases, the samples have low carbon content and less liquid phase is expected to form during sintering. Notwithstanding, the behavior is similar: Cu additive promotes sintering according the smaller activation energy. Also, the absent of C seems to be beneficial for the sintering process of Ni–YSZ at high temperature since the activation energy is noticeably smaller compared to Fig. 7.

The evaluation of n parameter at Table 1 indicates the cermet sintering process is rather complex. The n parameter values are influenced by the particle shape and diffusion path [22]. Grain boundary diffusion control tends to exhibit lower n values, approaching 0.3, while lattice diffusion assumes 0.4. Sphere particles are said to increase the n values as well as complex diffusion paths that can occur at composites like the present case. The sample subjected to longer MA treatment period (8 h) seems to display lower n values due to large surface development, which may favor grain boundary diffusion. On the other hand, Cu addition brings more complexity to diffusion paths and contact patterns, leading to increasing n values when using PTFE vial. Sintered pellets microstructure SEM-BSE images in Fig. 10 give evidence of liquid phase sintering occurrence, as expected by Cu low melting point. This fact can lead to promotion of sintering, reducing both n values

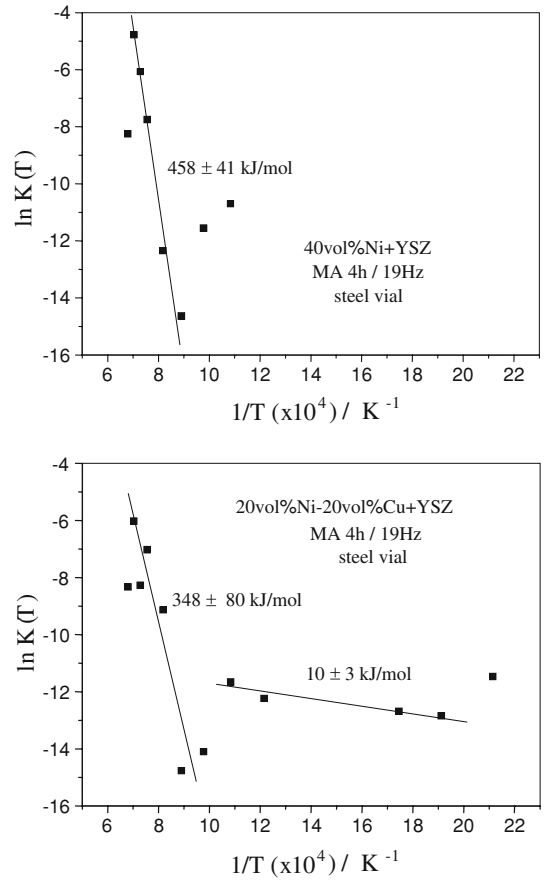

Fig. 9 Sintering activation energy for powder compacts milled in steel vial

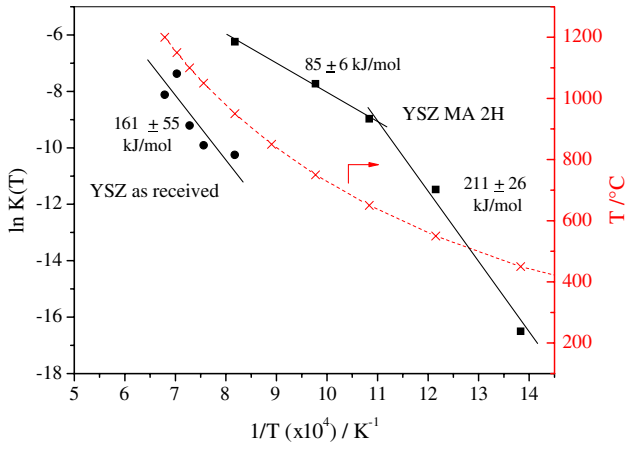

Fig. 8 Activation energies determined for YSZ row material as received and MA 2H

and the apparent activation energy for diffusion, as seen for the cermet processed in steel vial. However, it is found the YSZ material presently used has itself complicated diffusion kinetics, yielding rather high n values and therefore influencing the actual measurements. The Tosoh YSZ round particle shape may lead to this behavior.

The whole SID analysis should consider both n and activation energy values to determine the sintering mechanisms. In this work, since the cermet material has several constituents and phases, one can evaluate the mechanisms based on apparent activation energy owing to the predominant process. However, different reactions can take place simultaneously and may have some influence: solid phase diffusion,

Table 1 Approximated n parameter values determined by SID kinetic analysis

T/n values	Sintering onset °C	1st step	2nd step
Ni–YSZ homogenized	750	0.7	0.5
Ni–YSZ MA 8 h UHMW vial	200	0.6	0.3
Cu–Ni–YSZ MA 2 h PTFE vial	300	0.8	0.4
Ni–YSZ MA 4 h steel vial	650	–	0.5
Cu–Ni–YSZ 4 h steel vial	200	0.65	0.22–0.45
YSZ as received	950	–	0.7
YSZ MA 2H PTFE vial	450	0.6–0.9	–

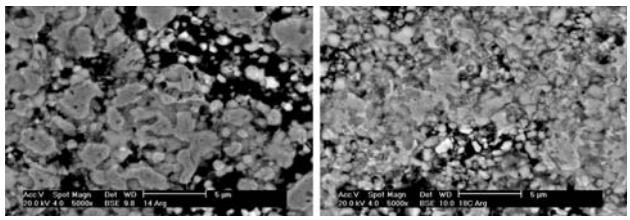

Fig. 10 SEM-BSE sintered pellets microstructure: Ni–YSZ (*left*) and Cu–Ni–YSZ (*right*); white-gray fields are YSZ-rich; liquid phase sintering is evident at the last sample

melting, solution-reprecipitation by liquid phase, formation of compounds, recovery, recristalization and grain growth. In spite of the system complexity, the present study can assure the densification process may occur through metal particles sintering at low temperature due to low activation energy determined, afterwards undergoing a mechanism change where the limiting rate process should include ceramic diffusion mechanisms. Moreover, the appearance of liquid phase (Cu) can promote the shrinkage accordingly to the respective lower apparent activation energy.

Conclusions

Cermet powder materials Ni(Cu)–YSZ for SOFC anode application were prepared by mechanical alloying with good dispersion and nanometric ultimate particle size. The MA powder pellets sintered in argon can lead directly to porous anode material with suitable microstructure. SID kinetic analysis has demonstrated the sintering occurs through a 2-step process: Ni(Cu) sintering at low temperature followed by YSZ sintering. Liquid phase sintering takes part in the process, accelerating the densification. Determined activation energies validate such behavior and confirm the Cu additive promotes sintering. The kinetic parameter n suggests the diffusion path and particle contact patterns are complex for the multi-component cermet and also verified for YSZ. The MA into steel vials can lead to a carbon-free cermet, which has an even higher sinterability.

References

1. Minh NQ. Ceramic fuel cells. J Am Ceram Soc. 1993;76(3); 563–88.
2. Atkinson A, Barnett S, Gorte RJ, Irvine JT, McEvoy AJ, Mogensen M, et al. Advanced anodes for high temperature fuel cells. Nat Mater. 2004;3(1):17–27.
3. Maèek J, Novosel B, Marinšek MJ. Ni–YSZ SOFC anodes—minimization of carbon deposition. J Eur Ceram Soc. 2007;27 (2–3):487–91.
4. Sankar J, Xu Z, Yarmolenko S. FY 2005 Progress Report for Heavy Vehicle Propulsion Materials, 4D. Processing and Characterization of Structural and Functional Materials for Heavy-Vehicle Applications, 89–97 (May 2006).
5. Sun C, Stimming UJ. Recent anode advances in solid oxide fuel cells. J Power Sources. 2007;171(2):247–60.
6. Gross MD, Vohs JM, Gorte RJ. A study of thermal stability and methane tolerance of Cu-based SOFC anodes with electrodeposited Co. Electrochim Acta. 2007;52(5):1951–7.
7. Guisard Restivo TA, Mello-Castanho SRH. $YZrO_2$-Ni cermet processing by high energy milling. Mater Sci Forum. 2008;591–593:514–20.
8. Sorensen OT. Thermogravimetric and dilatometric studies using Stepwise Isothermal Analysis and related techniques. J Therm Anal. 1992;38(1–2):213–28.
9. Husum PL, Sorensen OT. Computer controlled forced stepwise isothermal analysis. Thermochim Acta. 1987;114:131–8.
10. Guedes E Silva CC, Carvalho FMS, Restivo TAG. Estudo dos Mecanismos de Difusão em Cerâmicas a Base de Alumina. In: 14ª Congresso Brasileiro de Ciência e Engenharia de Materiais, Águas de São Pedro, SP, Brasil, dez. 2000.
11. Restivo TAG, Pagano L Jr. Sintering studies on the $UO_2 \cdot Gd_2O_3$ system using SID method, In: Conference on characterization and quality control of nuclear fuels 2002, Hyderabad, India, 2003.
12. Restivo TAG, Pagano L Jr. Effect of additives on the sintering kinetics of the $UO_2 \cdot Gd_2O_3$ system, In: TCM Brussels, Oct 2003.
13. El Sayed Ali M, Sorensen OT. Riso-R-518, 1985. 12p.
14. Wang H, Liu X, Chen F, Meng G, Sorensen OT. Kinetics and mechanism of a sintering process for macroporous alumina ceramics by extrusion. J Am Ceram Soc. 1998;81(3):781–4.
15. Bellon O. Dilatometric sintering studies of zirconia toughened ceramics. Centre for Advanced Technical Ceramics. Ecole Nationale Superieure de Ceramiques Industrielles. Risoe National Laboratory. 1991.
16. Yan R, Chu F, Ma Q, Liu X, Meng G. Sintering kinetics of samarium doped ceria with addition of cobalt oxide. Mater Lett. 2006;60(29–30):3605–9.
17. Restivo TAG, Mello-Castanho SR, Cu-Ni-YSZ anodes for solid oxide fuel cell by mechanical alloying processing In: 7th Internation Workshop on Interfaces Santiago de Compostela, Spain, 2008, ISBN 9788498601015.
18. Ashby MF, Bahk S, Bevk J, Turnbull D. The influence of a dispersion of particles on the sintering of metal powders and wires. Prog Mater Sci. 1980;25:1–34.
19. Panigrahi BB. Sintering and grain growth kinetics of ball milled nanocrystalline nickel powder. Mater Sci Eng A. 2007;460–461:7–13.
20. Zhou YH, Harmelin M, Bigot J. Preparation of ultra-fine metallic powders. A study of the structural transformations and of the sintering behaviour. Mater Sci Eng A. 1991;113:775–9.
21. Tanaka T, Ishihara KN, Shingu PH. Formation of metastable phases of Ni-C. Metall Mater Trans A. 1992;23(9):2431–5.
22. Jianlong Y. Technical Report, Centre for Advanced Technical Ceramics, Riso National Laboratory, July 1993.